Journal of Crystal Growth 69 (1984) 421–441
North-Holland, Amsterdam

CRITICAL ANALYSIS AND OPTIMIZATION OF THE THERMODYNAMIC PROPERTIES AND PHASE DIAGRAMS OF THE III–V COMPOUNDS
II. The Ga–As and In–As systems

Mohamed TMAR, Armand GABRIEL, Christian CHATILLON and Ibrahim ANSARA

Laboratoire de Thermodynamique et Physico-Chimie Métallurgiques (LTPCM), Associé au CNRS, LA 29, ENSEEG, Domaine Universitaire, BP 75, F-38402 Saint Martin d'Hères Cedex, France

Received 7 July 1984; manuscript received in final form 10 October 1984

A critical assessment of thermodynamic and phase diagram data for the Ga–As and In–As systems has been performed by first carrying out a complex chemical equilibrium analysis of the conditions of measurements, then performing a critical analysis of all the experimental methods employed, and finally, after eliminating those results which seem erroneous or which show systematic deviation, and reevaluating the experimental accuracies, by optimizing the retained data together. The best self-consistent values obtained are the following: ΔH_f°(GaAs, s, 298 K) = -19.54 ± 0.30 kcal mol^{-1}, S_{298}°(GaAs, s) = 16.05 ± 0.80 cal K^{-1} mol^{-1}, L_f(GaAs, s $\rightarrow$ l) = 27.0 ± 0.80 kcal mol^{-1} at $T_f = 1513.5 \pm 3$ K, ΔH_f°(InAs, s, 298 K) = -14.29 ± 0.50 kcal mol^{-1}, S_{298}°(InAs, s) = 17.84 ± 0.80 cal K^{-1} mol^{-1}, L_f(InAs, s $\rightarrow$ l) = 19.04 ± 1.00 kcal mol^{-1} at $T_f = 1212 \pm 3$ K. The Gibbs energies of formation for the compounds are represented by the equations: ΔG_f°(GaAs, s) = $-19537 + 1.849T$ cal mol^{-1}, ΔG_f°(InAs, s) = $-14291 + 2.257T$ cal mol^{-1}. Optimized partial pressures of In, Ga, As_2, As_4, InAs and GaAs molecules and phase diagrams have been obtained.

1. Introduction

A precise knowledge of the thermodynamic properties and phase diagrams of III–V compounds is very important for the monitoring of single crystal growth, the control of liquid phase epitaxy reactors and the calculation of chemical vapor deposition processes. A theoretical evaluation of the chemical processes may be performed when the thermodynamic properties of the main components are available. Moreover, a part from this direct application to the manufacturing process, if all thermodynamic properties are available, the calculation of impurity concentrations is possible, and substrate degradation may also be avoided by the choice of suitable atmospheric compositions in the epitaxy furnaces. In addition, the vaporization processes of III–V compounds can be well described and the experimenter may thus calculate flows of gaseous molecules in molecular beam epitaxy as well as the flow conditions leading to deposits on the targets.

The aim of this contribution is to establish by means of an optimization technique the most consistent set of thermodynamic and phase diagram data resulting from selected experimental values which are obtained from thermodynamic and methodological analysis of the experiments. The general method of analysis of the experimental observations has been used previously for the In–P and Ga–P systems [1] and will be applied here to the In–As and Ga–As systems. The first step is an analysis of the partial pressures of arsenic species in the gaseous phase, since there is disagreement concerning the composition of arsenic vapor.

2. Thermodynamics of the vaporization of arsenic

When As or its compounds vaporize, the main gaseous species are As_4 and As_2. The total pressure of the gaseous phase in equilibrium with pure solid As is accurately known, as shown by comparing the values from different compilations [2–4]; however the tabulated composition of the gaseous phase shows large discrepancies. Indeed, the dis-

0022-0248/84/$03.00

Table 1
Selected values for pure As

Species	ΔH_f°(298 K) (kcal/mol)	S_{298}° (cal/K·mol)	$H_{298}^\circ - H_0^\circ$ (cal/mol)	$C_p = a + bT + cT^2 + dT^{-2}$ (cal/mol)			
				a	b	c	d
$As_2(g)$	45.58 (±0.200) [4]	57.546 [3]	2252 [3]	8.772	2.751×10^{-4}	-1.21×10^{-7}	-4.241×10^{4}
$As_4(g)$	36.725 (±0.400) [4]	78.232 [3]	4192 [3]	19.696	2.834×10^{-4}	-1.252×10^{-7}	-1.68×10^{5}
As(s)	0 [4]	8.53	1223	5.55	1.298×10^{-3}	0	-5.55×10^{3}
As(l)	Our selected value			6.95	0	0	0

N.B.: $L_f(As) = 5842$ cal (Kaufman et al. [10]) and $T_f = 1090$ K (Rau [9]).

sociation energy of As_4 into As_2 varies from 82.5 to 59.9 kcal/mol [3]. Recently Pottie and coworkers [5,6] and Drowart et al. [7] redetermined mass spectrometrically this energy and both found a value close to 54.4 kcal/mol, while Vigdorovich et al. [8] report a value of 52.7 kcal/mol obtained from vapor density measurements. Drowart et al.'s value is selected in this analysis (see table 1) and allows the recalculation of the composition of the vapor phase in equilibrium with the III–V compounds from the total vapor pressure measurements.

The partial pressure values needed up to the melting temperatures of the compounds (GaAs and InAs), and simultaneously above pure arsenic, were derived from Rau's total vapor pressure measurements [9]. The value estimated by Kaufman et al. [10] for the enthalpy of fusion of arsenic has also been used. It is compatible with the value derived from Rau's measurements. The heat capacity of liquid As was taken as constant, the recalculated vapor pressure differing by a maximum of 6% from Rau's determinations. The thermodynamic data are listed in table 1.

In the optimization procedure for phase diagram and thermodynamic data, Gibbs energies of mixing or activity data are used. Hence it is important to evaluate the influence of the uncertainty associated with the equilibrium dissociation ($As_4 \rightleftharpoons 2As_2$) constant K on the final Gibbs energy of mixing. At any temperature, the partial pressure of gaseous As_2 in equilibrium with As_4 above the compound or the pure arsenic is:

$$P(As_2) = \frac{-K + \sqrt{K^2 + 4KP_T}}{2}, \tag{1}$$

where P_T is the total measured pressure. The uncertainty associated with K and P_T is:

$$dP(As_2) = -\frac{dK}{2} + \frac{2K\,dK + 4P_T\,dK + 4K\,dP_T}{4\sqrt{K^2 + 4KP_T}}. \tag{2}$$

As an example, in table 2 the uncertainty in the partial Gibbs energy of As in the two-phase In + InAs region is given at 1100 and 1200 K, assuming an uncertainty of ±10% when measuring P_T and

Table 2
Uncertainty in the partial Gibbs energy of mixing of As using for the total pressure experimental accuracies $\Delta P/P = \pm 10\%$, and an uncertainty of ±2000 cal for the dissociation energy of $As_4 \rightleftharpoons 2As_2$; application to the InAs compound

T (K)	$\delta P(As_2)/P(As_2)$ over In + InAs	$\delta P^\circ(As_2)/P^\circ(As_2)$ over pure As	$\delta(\overline{\Delta G}_{As})$ (cal)
1100	0.188 [a]	0.25	−156
	0.252 [a]	0.25	+5
1200	0.206 [a]	0.24	−93
	0.235 [a]	0.24	−19

[a] These values are extreme values as deduced from published total pressures of the gaseous phase in equilibrium with In + InAs.

± 2000 cal for the standard enthalpy of dissociation. This shows that the influence of the uncertainty associated with the enthalpy dissociation is negligible when optimizing phase diagram and thermodynamic data. This uncertainty becomes more important when recalculating the absolute partial pressures of the As_4 and As_2 species above the Ga–As and In–As systems.

3. Thermodyanic and phase diagram data

3.1. Vapor pressure and activity determinations

Partial pressures of As_2 and/or As_4 and tentatively Ga or In have been measured by Knudsen-cell mass spectrometry [6,11–17,30,31]. To analyse the parasitic reevaporations, some authors used cryogenic panels [13,15,16], shutter profiles [5,6] or modulated beams with phase detection [15,16]. Total arsenic pressure measurements have been performed by static methods such as dew point techniques [18–20], also coupled with continuous weighing [21,32], Bourdon gauges [8,22] and dynamic methods such as transport by H_2 flow [24,25,33] or equilibrium with $H_2 + AsH_3$ flows [26]. At low temperatures electro-chemical methods (EMF) were used to determine the activities of Ga or In in the two-phase region GaAs–As or InAs–As [27–29,34]. Tables 3 and 4 present the experimental information for the Ga–As and In–As systems respectively.

Table 3
Published vapor pressure or activity measurements in the Ga–As systems

System	Cell or crucible material	Method of measurement	Temperature range (K)	Reference
GaAs [a)]	Graphite	Knudsen-cell mass spectrometry	1030–1136	Drowart and Goldfinger [11]
GaAs	Graphite	Knudsen-cell mass spectrometry	1065–1165	Gutbier [12]
GaAs	Quartz	Knudsen-cell mass spectrometry	890–1190	Arthur [13]
GaAs	Graphite	Knudsen-cell mass spectrometry	1106–1197	De Maria et al. [14]
GaAs	?	Knudsen-cell mass spectrometry and modulated molecular beam	1030–1180	Foxon et al. [15]
GaAs	?	Knudsen-cell mass spectrometry and modulated molecular beam	–	Foxon et al. [16]
GaAs	Graphite	Knudsen-cell mass spectrometry with shutter profile	1035–1239	Pupp et al. [6]
GaAs	?	Knudsen-cell mass spectrometry	1000–1300	Rubinshteiin et al. [17]
GaAs	Quartz and graphite	Dew point	1054–1508	Van den Boomgaard and Schol [18]
GaAs	Quartz	Vapor density and microscopic observation	Melting temperature	Folberth [19]
Ga–GaAs	Quartz	Dew point	1324–1469	Lyons and Silvestri [20]
Ga–As	Quartz	Dew point and continuous weighing	1448–1511	Rakov et al. [21]
Ga–GaAs	Quartz	Bourdon gauge	1316–1531	Richman [22]
Ga–GaAs	Quartz	Bourdon gauge	1253–1353	Vigdorovich et al. [8]
Ga–GaAs	Quartz + graphite + molybdenum	Transport of As_2 and As_4 in a H_2 flow	973–1273	Khukhryanskii et al. [24,25]
Ga–GaAs	Quartz	Equilibrium with a $H_2 + AsH_3$ flow	1255–1435	Panish [26]
GaAs–As	–	Electromotive force (EMF) measurements	637–741	Abbasov et al. [27]
GaAs–As	–	Electromotive force (EMF) measurements	638–741	Krestovnikov et al. [28]
GaAs–As	–	Electromotive force (EMF) measurements	683–743	Sirota [29]

[a)] When measuring the vaporisation of the compound GaAs at high temperature, a non-congruent evaporation occurs and the pressure measurements are effectively performed over the Ga(l)+GaAs(s) system.

Table 4
Published experimental vapor pressure or activity measurements in the In–As system

System	Container material	Method of measurement	Temperature range (K)	Reference
InAs [a)]	Graphite	Knudsen-cell mass spectrometry	1020–1060	Gutbier [30]
InAs	Graphite	Knudsen-cell mass spectrometry	≈ 1050	Gutbier [12]
InAs	Graphite	Knudsen-cell mass spectrometry	911–1159	Goldfinger and Jeunehomme [31]
In–InAs	Graphite	Knudsen-cell mass spectrometry with a shutter profile	918–1084	Pupp et al. [6]
InAs	Quartz and graphite	Dew Point	1004–1215	Van den Boomgaard and Schol [18]
In–As	Quartz	Dew point and continuous weighing	1149–1220	Karataev et al. [32]
InAs	Quartz	Vapor density and microscopic observation	Melting temperature	Folberth [19]
InAs	Quartz + graphite	Transport of As_2 and As_4 in a H_2 flow	973–1100	Khukhryanskii et al. [25]
In–As	Quartz + graphite	Transport of As_2 and As_4 in a H_2 flow	1058–1133	Khukhryanskii and Panteleev [33]
InAs–As	–	Electromotive force (EMF) measurements	513–783	Abbasov et al. [34]
InAs–As	–	Electromotive force (EMF) measurements	633–784	Krestovnikov et al. [28]

[a)] The vaporization of the InAs compound being incongruent, the measurements performed on the InAs compound relate in fact to two-phase In + InAs mixtures.

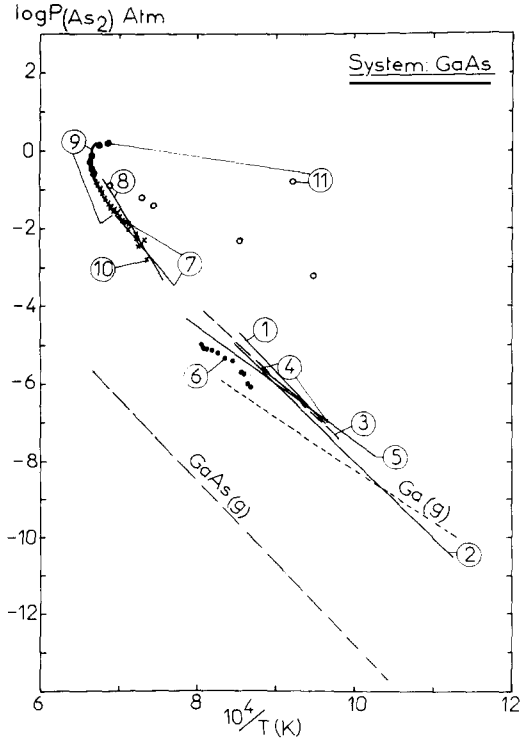

In order to compare all the published results, excluding those obtained at low pressure by mass spectrometry or by EMF, the partial pressures of As_2 and As_4 have been recalculated using the basic data established previously, in section 2, for As. This also allows total pressures derived from dew-point determinations [18–21,32] to be recalculated. These corrected experimental results are compared with each other in figs. 1 and 2. The measurements relative to Ga–As are only slightly scattered, whereas those fewer concerning In–As, show large discrepancies.

3.2. Calorimetric and heat content determinations

Enthalpies of reaction, as well as enthalpy and entropy values for the GaAs and InAs com-

Fig. 1. Logarithm of the As_2 vapor pressure in equilibrium with the two-phase mixtures liquid phase + GaAs compound: (1) Foxon et al. [15]; (2) Arthur [13]; (3) Pupp et al. [6]; (4) Drowart and Goldfinger [11]; (5) Khukhryanskii et al. [24,25]; (6) De Maria et al. [14]; (7) Panish [26]; (8) Lyons and Silvestri [20]; (9) Rakov et al. [21]; (10) Richman [22]; (11) Van den Boomgaard and Schol [18]. The Ga and GaAs pressures are also presented. The Ga pressure corresponds to the Ga-rich side of the two-phase mixtures.

Table 5
Published experimental calorimetric and enthalpy data for the GaAs compound

Thermodynamic data	Value	Experimental technique	Reference
Enthalpy of formation (kcal mol^{-1})	$\Delta H_f^\circ(523\ K) = -19.69 \pm 0.32$	Calorimetric precipitation	Martosudirjo and Pratt [35]
	$\Delta H_f^\circ(298\ K) \sim -20.96 \pm 1$	O_2 calorimetric bomb	Sirota [29]
Entropy (cal K^{-1} mol^{-1})	$S_{298}^\circ = 15.34 \pm 0.1$	Thermometry	Piesbergen [36]
		Thermometry	Holste [37]
Heat capacity (cal K^{-1} mol^{-1})	$C_p = 10.80 + 14.6 \times 10^{-4} T$ (298–1250 K)	Drop calorimetry	Cox and Pool [38]
	$C_p = 10.70 + 2.32 \times 10^{-3} T$ (310–980 K)	Differential Scanning Calorimetry	Dash et al. [39]
	$C_p = 11.33 + 16.63 \times 10^{-4} T$ (421–1513 K)	Drop calorimetry	Lichter and Sommelet [40]
Enthalpy of fusion (kcal mol^{-1})	$L_f = 21 \pm 5$ ($T_f = 1518 \pm 5$ K)	Differential Thermal Analysis	Richman and Hockings [41]
	$L_f = 25.18 \pm 0.60$ ($T_f = 1513 \pm 1$ K)	Drop calorimetry	Lichter and Sommelet [40]

Table 6
Published experimental calorimetric and enthalpy data for the InAs compound

Thermodynamic data	Value	Experimental technique	Reference
Enthalpy of formation (kcal mol^{-1})	$\Delta H_f^\circ(298\ K) = -14.8 \pm 0.12$ (s.d.)	Dissolution calorimetry	Schottky and Bever [42]
	$\Delta H_f^\circ(298\ K) = -13.8 \pm 0.8$	Calorimetric bomb	Sharifov et al. [43]
Entropy (cal K^{-1} mol^{-1})	$S_{298}^\circ = 18.1 \pm 0.10$	Thermometry	Piesbergen [36]
		Thermometry	Holste [37]
Heat capacity (cal K^{-1} mol^{-1})	$C_p = 10.6 + 2 \times 10^{-3} T$ (298–1200 K)	Drop calorimetry	Cox and Pool [38]
	$C_p = 11.822 + 2.026 \times 10^{-3} T$ (298–1200 K)	Drop calorimetry	Lichter and Sommelet [40]
Enthalpy of fusion (kcal mol^{-1})	$L_f = 18 \pm 6$ ($T_f = 1215 \pm 3$ K)	Differential Thermal Analysis	Richman and Hockings [41]
	$L_f = 17.58 \pm 0.40$ ($T_f = 1210 \pm 1$ K)	Drop calorimetry	Lichter and Sommelet [40]

Table 7
Experimental techniques used to determine the Ga–As phase diagram

Concentration range (mole fraction As)	Temperature range (K)	Cell or crucible material	Experimental technique	Reference
0–1	300–1511	Quartz	Differential Thermal Analysis	Goldsmith in Koster and Thoma [44]
0–0.07	685–905	–	–	Hsieh [23]
0–0.1	723–1300	Quartz + H_2 flow	Heterogeneous equilibrium and single-crystal weight loss	Hall [45]
0.5	1518 ± 5	Quartz	Differential Thermal Analysis	Richman and Hockings [41]
0–0.4	973–1473	Quartz	Filtration technique	Rubenstein [46]
0.3–0.6	1448–1511	Quartz	Dew point with continuous weighing	Rakov et al. [21]
0–0.03	1013–1121	Quartz + graphite + H_2 flow	Heterogeneous equilibrium in a Liquid Phase Epitaxy (LPE) reactor and weight loss of a single crystal	Sol et al. [47]
0–0.22	1253–1353	Quartz	Bourdon gauge and vapor density	Vigdorovich et al. [8]
0–0.003	879–915	Quartz + graphite + H_2 flow	Heterogeneous equilibrium in a LPE reactor and weight loss of a single crystal	Perea and Fonstad [48]
0.0056–0.058	965–1173	Quartz + H_2 flow	Visual observation of crystals	Dutartre [59]

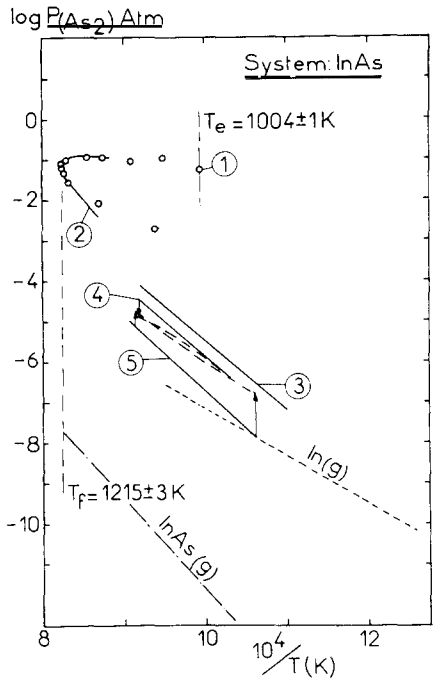

Fig. 2. Logarithm of the As_2 vapor pressure in equilibrium with the two-phase mixtures liquid phase + InAs compound: (1) Van den Boomgaard and Schol [18]; (2) Karataev et al. [32]; (3) Pupp et al. [6]; (4) Khukhryanskii et al. [25]; (5) Goldfinger and Jeunehomme [31]. The dashed lines with arrows are corrections applied to values from refs. [4] and [5] as explained in sections 4 and 5 of the text. The In and InAs pressures are also presented. The In pressure corresponds to the In-rich side of the two-phase mixtures.

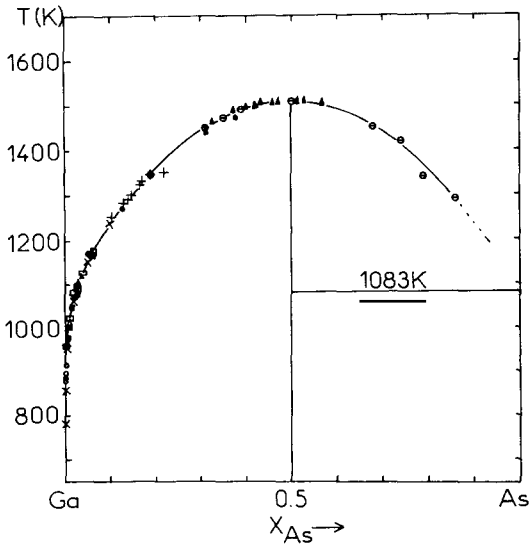

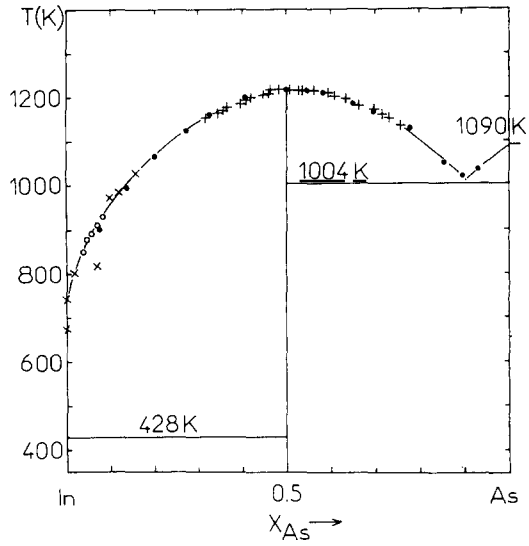

Fig. 4. In–As phase diagram as experimentally determined: (×) Hall [45]; (○) Perea and Fonstad [48]; (●) Liu and Peretti [49]; (+) Karataev et al. [32].

pounds, have been derived from calorimetric measurements [29,35–46]. Tables 5 and 6 list the derived heats of formation, entropy and heat content values together with the experimental techniques used. For the GaAs compound, three determinations of the heat capacity show large discrepancies. For the InAs compound the results of Cox and Pool [38] and Lichter and Sommelet [40] are slightly different when approaching the melting point.

3.3. Phase diagram determinations

The Ga–As and In–As phase diagrams are characterized by the existence of the congruent melting compounds (when melting under their own pressure) GaAs and InAs, and virtually no mutual solubility between the pure solid constituents. The liquidus temperature has been determined up to the melting point by various techniques, as listed in tables 7 and 8. The results show general agree-

Fig. 3. Ga–As phase diagram as experimentally determined: (×) Hall [45]; (●) Rubenstein [45]; (⊖) Koster and Thoma [44]; (+) Vigdorovich et al. [8]; (▲) Rakov et al. [21]; (△) Sol et al. [47]; (○) Perea and Fonstad [48]; (■) Dutartre [59]; (□) Hsieh [23].

Table 8
Experimental techniques used to determine the In–As phase diagram

Concentration range in x_{As}	Temperature range (K)	Cell or crucible material	Experimental technique	Reference
0–1	429–1215	Vycor + Ar atm. or sealed quartz	Differential Thermal Analysis and X-ray analysis	Liu and Peretti [49]
0–0.16	673–1024	Quartz + H_2 flow	Heterogeneous equilibrium and weight loss of a single crystal	Hall [45]
0.35–0.74	1149–1220	Quartz	Dew point and continuous weighing	Karataev et al. [32]
0–0.08	849–929	Quartz + graphite + H_2 flow	Heterogeneous equilibrium in a LPE reactor and weight loss of a single crystal	Perea and Fonstad [48]

ment, except for the the Ga–As results deduced from Koster and Thoma [44], as shown in figs. 3 and 4. Generally, the compositions close to pure As have not been investigated.

4. Thermodynamic analysis of the data and of their conditions of measurements

An analysis of the vapor pressure measurements by means of the 2nd and 3rd laws of thermodynamics leads to mean values of S°_{298} and $\Delta H^\circ_{f,298\,K}$ for the compounds InAs and GaAs. These values are then used in a complex equilibrium calculation in order to analyse the actual measurements in relation to their environmental conditions, i.e. to determine whether parasitic chemical reactions or transport phenomena occur. These different steps are described below.

4.1. Application of the 2nd and 3rd laws of thermodynamics

The chemical equilibria studied in the Ga–As and In–As systems are the following:

$$As_4(g) \rightleftharpoons 2\,As_2(g), \tag{3}$$

$$Ga(l) + \tfrac{1}{2}As_2(g) \rightleftharpoons GaAs(s), \tag{4}$$

$$Ga(l) + \tfrac{1}{4}As_4(g) \rightleftharpoons GaAs(s), \tag{5}$$

$$Ga(l) \rightleftharpoons Ga(g), \tag{6}$$

$$Ga(ss) + As(s) \rightleftharpoons GaAs(s), \tag{7}$$

$$In(l) + \tfrac{1}{2}As_2(g) \rightleftharpoons InAs(s), \tag{8}$$

$$In(l) + \tfrac{1}{4}As_4(g) \rightleftharpoons InAs(s), \tag{9}$$

$$In(l) \rightleftharpoons InAs(s), \tag{10}$$

$$In(ss) + As(s) \rightleftharpoons InAs(s), \tag{11}$$

where (g) is used for gas, (l) for liquid, (s) for solid and (ss) for solid solution.

Since the heteronuclear molecules whose thermodynamic properties have been determined under different experimental conditions (GaAs [14] and InAs [50]), also exist, the corresponding equilibria:

$$\text{pure } GaAs(s) \rightleftharpoons GaAs(g),$$

$$\text{pure } InAs(s) \rightleftharpoons InAs(g)$$

were calculated. As may be observed in figs. 1 and 2, these molecules do not modify the total pressure measurements significantly, but their presence can be detected by mass spectrometry when vaporizing GaAs or InAs.

An analysis by means of the 2nd and 3rd laws involves a knowledge of the thermal functions for As_2 and As_4 as calculated previously (section 1). Hultgren et al.'s data [3] were selected for In (s), (l) or (g) and for Ga (s), (l) or (g). For the GaAs and InAs compounds the thermal functions are established from heat capacity measurements:

– GaAs: a good agreement between refs. [39,40] and [36] is observed, but a difference remains between the values of these authors and those of Cox and Pool [38]. No explanation is apparent. The discrepancies may be due to interaction between As and the Ta container, as indicated by the appearance of a compound in the phase diagram,

Table 9
2nd and 3rd law analysis of vapor pressure and EMF measurements in the Ga–As system

Reaction	Temperature range (K)	ΔH_T° (2nd law) (kcal mol^{-1})	ΔH_{298}° (kcal mol^{-1})		ΔH_f°(298 K) (3rd law) (kcal mol^{-1})	Reference
			2nd law	3rd law		
Ga(l)+$\frac{1}{2}$ As_2(g)	1291–1435	−24.98 (1362 K)	−25.64	−43.53±1.12	−20.74	Panish [26]
⇌ GaAs(s)	976–1269	−35.80 (1123 K)	−35.83	−43.67±0.9	−20.88 [a]	Khukhryanskii [24]
	1135–1170	−44.22 (1096 K)	−44.18	−43.13±0.29	−20.34	Foxon et al. [15]
	1019–1238	−44.14 (1134 K)	−44.20	−43.44±0.05	−20.65	Pupp et al. [6]
	1324–1469	−77.61 (1401 K)	−78.38	−41.76±1.32	−18.97 [a]	Lyons and Silvestri [20]
	1031–1136	−34.87 (1087 K)	−34.81	−43.31±0.52	−20.52	Drowart and Goldfinger [11]
	888–1190	−46.20 (1049 K)	−46.05	−43.84±0.22	−21.05	Arthur [13]
	1358–1511	−70.83 (1459 K)	−71.77	−41.41±1.02	−18.65 [a]	Richman [22]
	1358–1511	−69.99 (1450 K)	−61.90	−41.33±0.86	−18.54 [a]	Richman [22]
	1412–1508	−73.03 (1472 K)	−74.00	−41.10±0.85	−18.31 [a]	Richman [22]
	1435–1512	−110.53 (1487 K)	−111.56	−40.09±1.55	−17.30 [a]	Rakov et al. [21]
	1000–1300	−84.2 (1150 K)	−84.2			Rubinshteiin et al. [17]
	1054–1458	−24.31 (1393 K)	−25.65	−38.44±1.72	−15.65 [a]	Van den Boomgaard and Schol [18]
	1106–1197	−37.51 (1152 K)	−38.85	−44.20±0.28	−21.41	De Maria et al. [14]
Ga(l)+$\frac{1}{4}$$As_4$(g)	1324–1469	−64.47 (1401 K)	−64.71	−28.15±1.31	−18.97 [a]	Lyons and Silvestri [20]
⇌ GaAs(s)	1031–1136	−17.87 (1087 K)	−17.43	−26.04±0.37	−16.86	Drowart and Goldfinger [11]
	888–1190	−31.61 (1093 K)	−31.17	−28.59±0.14	−19.41	Arthur [13]
	1358–1511	−55.57 (1459 K)	−55.95	−27.83±0.97	−18.65 [a]	Richman [22]
	1358–1511	−48.20 (1450 K)	−48.55	−27.77±0.86	−18.59 [a]	Richman [22]
	1412–1508	−59.80 (1472 K)	−60.21	−27.54±0.84	−18.36 [a]	Richman [22]
	1435–1512	−95.93 (1487 K)	−96.37	−26.52±1.53	−17.34 [a]	Rakov et al. [21]
	1000–1300	−88.5 (1150 K)	−88.1			Rubinshteiin et al. [17]
	1054–1458	−11.04 (1393 K)	−12.37	−24.84±1.74	−15.66 [a]	Van den Boomgaard and Schol [18]
	1106–1197	−16.99 (1152 K)	−18.33	−26.50±0.31	−17.32	De Maria et al. [14]
As_4(g)	1324–1469	52.54 (1401 K)	54.69	54.46±0.28		Lyons and Silvestri [20]
⇌ 2 As_2(g)	1031–1136	67.98 (1087 K)	69.51	69.08±0.94		Drowart and Goldfinger [11]
	888–1190	56.74 (1093 K)	58.28	60.65±0.57		Arthur [13]
	1358–1511	61.05 (1459 K)	63.32	54.44±0.76		Richman [22]
	1358–1511	51.16 (1450 K)	53.40	54.24±0.12		Richman [22]
	1412–1508	59.80 (1472 K)	62.09	54.21±0.12		Richman [22]
	1435–1512	58.39 (1487 K)	60.69	54.29±0.22		Rakov et al. [21]
	1106–1197	79.0 (1152 K)	80.65	70.76±0.45		De Maria et al. [14]
	1054–1458	53.08 (1393 K)	55.23	54.36±0.14		Van den Boomgaard and Schol [18]
				54.40±2.00		Our retained value (section 2)
Ga(l) ⇌ Ga(g)	1135–1170	63.07 (1141 K)		64.72±0.02		Foxon et al. [15]
	1019–1238	62.07 (1126 K)		64.18±0.06		Pupp et al. [6]
	888–1190	63.42 (1033 K)		65.35±0.12		Arthur [13]
Compilation value	–	–	–	65.0±0.5	–	Hultgren et al [3]
Ga(ss)+As(s)	637–741	−19.91 (689 K)	−18.57	−17.47±0.15	−17.47±0.15	Abbasov et al. [27]
⇌ GaAs(s)	638–741	−21.31 (684 K)	−19.97	−16.83±0.15	−16.83±0.15	Krestovnikov et al. [28]
	683–743	−22.12 (713 K)	−20.78			Sirota [29]

[a] These high temperature measurements were not used to calculate the mean value of the standard enthalpy of formation for GaAs, the activity of Ga being far from unity.

Table 10
2nd and 3rd law analysis of the vapor pressure and EMF measurements in the In–As system

Reaction	Temperature range (K)	ΔH_T° (2nd law) (kcal mol^{-1})	ΔH_{298}° (kcal mol^{-1})		ΔH_f°(298 K)	Reference
			2nd	3rd law		
In(l)+$\frac{1}{2}$ As_2(g)	918–1083	−40.15 (1000 K)	−40.63	−37.37±0.21	−14.58	Pupp et al. [6]
⇌ InAs(s)	1136–1215	−12.12 (1192 K)	−13.11	−19.48±0.12	−10.31	Karataev et al. [32]
	1004–1201	+1.76 (1156 K)	+0.98	−31.74±2.10	−8.95	Van den Boomgaard and Schol [18]
	942–1098	−42.93 (1027 K)	−43.48	−40.30±0.27	−17.51	Goldfinger and Jeunehomme [31]
In(l)+$\frac{1}{4}$ As_4(g)	1136–1215	−12.79 (1192 K)	−12.24	−19.48±0.12	−10.30	Karataev et al. [32]
⇌ InAs(s)	1004–1201	−13.39 (1156 K)	−11.91	−18.16±2.04	−8.98	Van den Boomgaard and Schol [18]
As_4(g) ⇌ 2 As_2(g)	1136–1215	53.60 (1192 K)	55.33	54.50±0.06		Karataev et al. [32]
	1004–1201	48.85 (1156 K)	50.51	54.32±0.61		Van den Boomgaard and Schol [18]
				54.4±2.0	–	Selected value (see section 2)
In(ss)+As(s)	513– 783	−12.82 (648 K)	−12.04	−13.72±0.37	−13.72	Abbasov et al. [34]
⇌ InAs(s)	633– 784	−12.36 (707 K)	−11.58	−12.60±0.04	−12.60	Krestovnikov et al. [28]

and by analogy with the observation of Cox and Pool [38] in the case of liquid InAs. The value of S_{298}°, from Piesbergen [36], 15.34 ± 0.1 cal mol^{-1} K^{-1}, has been selected, as well as the mean value for C_p determined by Dash et al. [39] and by Lichter and Sommelet [40]: $C_p = 5.507 + 9.974 \times 10^{-4} T$ cal mol^{-1} K^1.

– InAs: high temperature C_p values [40,38] differ by about 9% at 1200 K. Just as for GaAs, Cox and Pool's [38] values are lower than those of Lichter and Sommelet [40], whose values were used to calculate the InAs thermal functions.

The 2nd and 3rd law analyses for reactions (3)–(11) are presented in tables 9 and 10. The calculations were performed on the recalculated original values or those obtained by EMF and mass spectrometry as presented in tables or graphs in original publications. The mean values for the enthalpies of formation of GaAs and InAs, obtained for rather low temperatures where the Ga or In activities are close to unity, are compared with calorimetric determinations as presented in tables 5 and 6. The values are generally in close agreement with values obtained by dissolution calorimetry. Finally, the calorimetric values of Martosudirjo and Pratt [35] are retained for GaAs, ΔH_f° (GaAs, s, 298 K) = −19.52 kcal/mol, and those of Schottky and Bever [42] for InAs, ΔH_f°(InAs, s, 298 K) = −14.8 kcal/mol. These values enable a preliminary set of thermodynamic functions to be established for GaAs and InAs for use in complex equilibrium analysis.

4.2. Complex equilibrium calculations for reactors

For measurements performed under static conditions such as vapor pressure measurements using a Bourdon gauge, or DTA with samples contained in sealed SiO_2 vessels, it is easy to analyse the contribution due to parasitic chemical reactions such as:

$$2\,GaAs(2) + SiO_2(s) \rightleftharpoons 2\,AsO(g) + 2\,Ga(l,s) + Si(l,s),$$

or

$$GaAs(s) + SiO_2(s) \rightleftharpoons AsO(g) + SiO(g) + Ga(l,s).$$

The JANAF data are used for SiO_2(s), SiO(g) and Si. In addition, the thermal functions for AsO(g) and the thermodynamic properties of Ga–Si or In–Si solutions are quoted in refs. [51] and [52] respectively. At 1500 K, for example, the calculated AsO gas pressure will be about 10^{-14} atm. The vapor pressures of SiO gas or other species have already been investigated [62] to explain the Si contamination of GaAs compounds. These pressures are very low. Thus we conclude that in

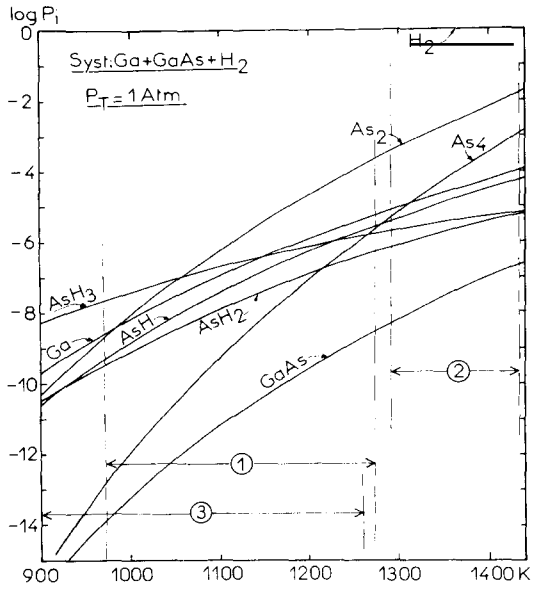

Fig. 5. Gaseous phase composition in equilibrium with the compound GaAs and a H_2 carrier gas at 1 atm: (1) temperature range of Khukhryanskii et al's measurements [24,25]; (2) Panish's flow technique [26]; (3) Hall's determinations [45].

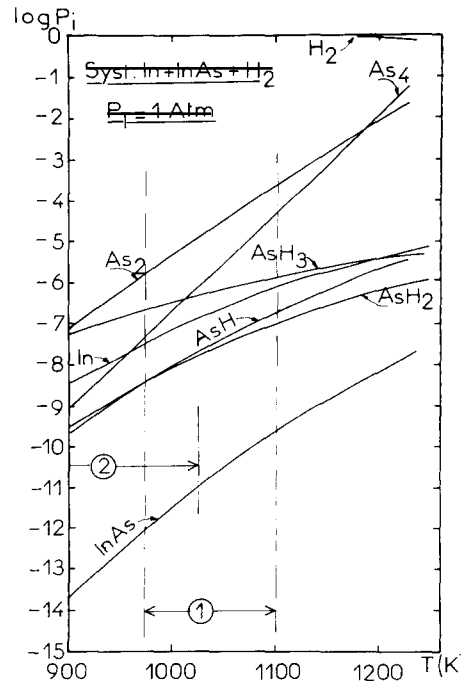

Fig. 6. Gaseous phase composition in equilibrium with the compound InAs and a H_2 carrier gas at 1 atm: (1) temperature range of Khukhryanskii et al's measurements [25]; (2) Hall's determinations [45].

static methods, no parasitic chemical reactions with the SiO_2 container can significantly modify the measured pressures.

For dynamic measurements, flows of H_2 or $H_2 + AsH_3$ mixtures may be transformed by chemical reactions with the container materials (SiO_2 or graphite) or also by chemical decomposition of some gaseous species. The influence of these different reactions may be tested or directly evaluated by using complex equilibrium calculations, the results being shown in figs. 5 and 6. These calculations are performed under equilibrium conditions which are theoretically obtained when the carrier gas flows reach a zero value. On the other hand, when high flow values are used, we can also qualitatively estimate the mass loss of the sample. From calculations carried out for InP or GaP compounds [1], we can conclude by analogy that:

(i) The assumption of Khukhryanskii et al. [24,25,33] that As_2 is the main vapor species is erroneous since As_4, AsH_3, AsH_2 and AsH gas also transport the As component. For the study relative to InAs [25], from the results shown in fig. 6, the mole ratio of arsenic transported by As_2 versus the total arsenic transported by $As_2 + As_4 + AsH_3 + AsH_2 + AsH$ is 0.886 at 973 K and 0.742 at 1073 K. For the GaAs compound [24,25], this ratio varies from 0.15 at 973 K to 0.97 at 1200 K and 0.976 at 1273 K. These variations are not proportional to T and the enthalpies derived from a second law analysis contain a summation of at least three partial vaporization reactions. These enthalpies are necessarily erroneous. As no experimental values are published, we cannot correct the original measurements with a complex equilibrium calculation to include them in the optimization analysis. For the activity of As [33], the situation is even worse, because when this quantity decreases, the As_2 pressure decreases more rapidly than the AsH_3 pressure. For these reasons the measurements of Khukhryanskii et al. [24,25,33] were discarded.

(ii) The vapor pressure measurements using the

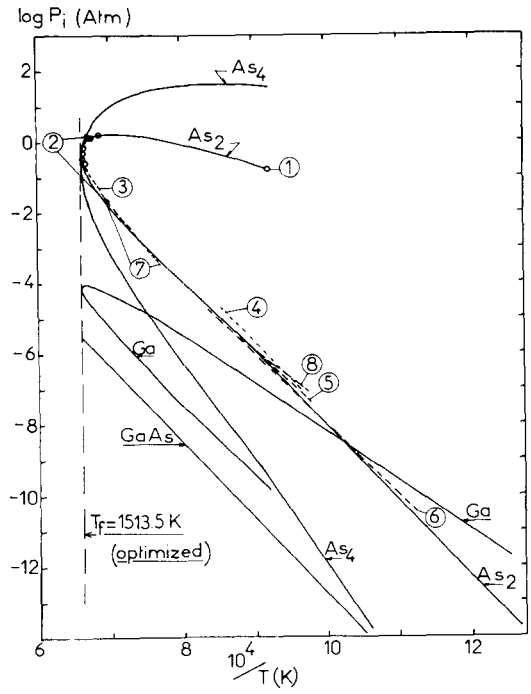

Fig. 7. Optimized partial pressures of As_2, As_4, Ga and GaAs gaseous species along the liquidus in the Ga–As system and selected experimental data: (1) Van den Boomgaard and Schol [18]; (2) Rakov et al. [21]; (3) Richman [22]; (4) Foxon et al. [15]; (5) Pupp et al. [6]; (6) Arthur [13]; (7) Panish [26]; (8) Drowart and Goldfinger [11].

$H_2 + AsH_3$ flow technique [26] were interpreted by the authors taking into account total decomposition of AsH_3 into $As_2 + As_4$ and H_2 gases. In this temperature range, the AsH_2, AsH molecules and residual AsH_3 are always $\approx 1\%$. Thus, it is not necessary to correct these original values. From a kinetic point of view as already evidenced by Ban [64], Panish's [26] measurements may be overevaluated. In fact, two reasons seem to indicate these measurements are performed close to equilibrium conditions. First, the flow rates in Panish's experiments were much smaller than those used by Ban (20 to 100 times). Second, Panish's [26] results finally will not be very different from other retained values (see fig. 7). We conclude that the As_2 and As_4 pressure values are not significantly overevaluated in Panish's [26] work.

(iii) Liquidus determinations in the Ga–As and In–As systems [45] may be erroneous due to As loss. This As loss comes from the reaction of H_2 flow with the sample and the bath producing the supplementary AsH_3, AsH_2 and AsH molecules. So, the total flow ($AsH_3 + AsH_2 + AsH + As_2 + As_4$) of arsenic, when rising along the laboratory tubing, is produced mainly as $AsH_3 + H_2$ flow, since the temperature decreases. Then, burning the outcoming gases, the main part of the As is lost in the atmosphere, while some residual As is deposited at the end of the tubing as observed by Hall [45]. Nevertheless, the loss of material is not so important as observed in the same apparatus with InP or GaP as reported by the author [45], but the liquidus composition may be slightly shifted towards the compounds. This shift will be larger in the Ga–As system, the As_2 pressure being higher in the temperature range of the measurements. These observations will be used later to evaluate the experimental uncertainties.

(iii) Schottky and Bever [42] made calorimetric measurements of a solution of InAs and an In + As mixture and suggested that the maximum uncertainty was due to monatomic arsenic vaporization during the calibration run. In fact the pure As vaporizes mainly as the tetra-atomic form $As_4(g)$. Taking into account this vaporization, the maximum error will lead to a more negative value of the enthalpy of formation ΔH_f (InAs, 298 K) = $-14.8 - 0.60 = -15.4$ kcal/mol. This error will be partly compensated (10% to 20%) by the vaporization of As_2 during the dissolution of the InAs compound. So the value -15.1 ± 0.7 kcal/mol has been chosen. This value is in agreement with the value measured by means of a bomb calorimeter [43]: -13.8 ± 0.8 kcal/mol.

5. Critical analysis of the methods of measurements

In all the different experimental techniques which have been used, some systematic errors may occur. As in the case of the In–P and Ga–P systems [1] these techniques are analyzed and the results which have been obtained are compared.

5.1. Knudsen-cell mass spectrometric measurements

The effect of parasitic phenomena and difficulties encountered with mass spectrometric measure-

ments were respectively analyzed for the parasitic reevaporation of arsenic, the dissociative ionization of As_4 into As_2^+, the reversibility of the evaporation process and the calibration of the mass spectrometer. A discussion of the experimental difficulties has been presented previously [1]. The general results of our analysis will be discussed together with the main observations made by different authors.

Parasitic reevaporation occurs mainly with the As_4 species, as shown by Foxon et al. [15], who used a modulated beam and a phase detection technique, by Arthur [13] with a cold trap, and by Pupp, Murray and Pottie [6] with both a cold trap and a shutter profile. By displacing the shutter, Arthur observed that evaporation of As_4 occurs in the ionization source. The As_4 source background is very difficult to eliminate as discussed previously [1]. The shutter profile used by Murray, Pupp and Pottie [5] ensures that the two species As_4 and As_2 do not have the same behavior. We have studied [53] the response of the ion source of a mass spectrometer shutter profile and demonstrated that it is very difficult to obtain quantitative values for reevaporation processes [53]. Comparing Pupp, Murray and Pottie's shutter profiles with our previous study [53], we can deduce that some parasitic contribution to As_4 and As_2 molecular flows occurred from the outer surface of the Knudsen-cell or from the shields. these contributions are quite large for As_4. This conclusion is probably valid for all the experimental investigations.

Dissociative ionization has been shown to occur during studies of the vaporization of pure As [6,54,30], and amounts to 7% to 18%, with the ionizing electron energy ranging from 40 eV to 70 eV. This contribution of $As_4(g)$ to the As_2^+ ionic current will be lower when the As_4 flow, mainly due to reevaporation is reduced. This will be the case when using a narrow cold trap around the source [13,6,15,16], the observed As_4 flow becoming lower than the As_2 flow.

The reversibility of the evaporation reaction is guaranteed only when the evaporating surface is large compared to the effusion area. This condition is fulfilled in the studies of De Maria et al. [14] and of Pupp, Murray and Pottie [6] but no details are given by Foxon et al. [15] and Arthur [13]. Goldfinger and Jeunehomme [31] vaporizing InAs and Drowart and Goldfinger [11] vaporizing GaAs, used an open crucible with a collimator diaphragm. Lou and Somorjai [55] measured an evaporation coefficient ($\alpha \simeq 1/6$) with a GaAs single crystal, but we cannot rule out the possibility of some coefficients being < 1 with grounded InAs or GaAs samples in these crucibles. The α values might be higher, because the non-congruent vaporization of these compounds produces Ga or In droplets or layers which can catalyze the vaporization, as already discussed by Gutbier [30].

The calibration of the mass spectrometer has been carried out using the As_2 ionic intensity integration and mass loss of the cells [11,13,6,14]. As the As_2 gaseous species is the most important, this calibration is probably the most accurate, and the reevaporation of As_4 is avoided. Goldfinger and Jeunehomme [31] and De Maria et al. [14] have calibrated their apparatus taking into account the two ionic species As_2^+ and As_4^+. If it is assumed that their As_4^+ ionic intensity is significantly overestimated due to parasitic reevaporation, such a calibration is erroneous. This excess of As_4^+ is demonstrated by the deduced value of their equilibrium dissociation constant ($As_4 \rightleftharpoons 2\ As_2$) which is far from the selected value in section 2. Recalculating the calibration constant with their sensitivity values, Goldfinger and Jeunehomme's value [31,32] are corrected, assuming As_2 as the main gaseous species, by a factor of 6.3 at 1000 K and 2.2 at 1100 K. These values are shifted towards Pupp, Murray and Pottie's [6] determinations. The same correction would pertain to De Maria et al.'s [14] values, decreasing the difference between these values and other determinations. As not enough information is available however, further corrections are not possible, and these values have not been retained. Foxon et al. [16] assumed that the sensitivity values are the same for Ga and As_2. This assumption is reasonable to within $\pm 50\%$.

In conclusion, we think that the determinations of As_2 pressures are the most accurate when using effusion cells and As_2 mass loss calibration as carried out by Arthur [13] and by Pupp, Murray and Pottie [6]. The estimate of Foxon et al. [16]

gives values which lie fortuitously in the range of other selected values. Goldfinger and Jeunehomme's [31] corrected values seem to be low when compared with Pupp, Murray and Pottie's results [6], probably because of an evaporation coefficient $\alpha < 1$, especially at high pressures with resulting high evaporating flow rate. Drowart and Goldfinger's [11] determinations over GaAs do not seem to be affected by such a process when compared with other determinations.

5.2. High pressure measurements

Higher pressure measurements are obtained mainly from dew-point techniques [18,20,19,32]. Richman [22] used quartz spoon gauges and differential manometers, and Vigdorovich et al. [23] a dynamic method with a quartz manometer. The dew-point technique presents certain difficulties, as has been indicated by these authors: the As may exist, at the dew-point site, in different allotropic states, the GaAs or InAs compound may form a layer at the surface of the liquid metal and the dew-point temperature, which is at a lower temperature, may be difficult to measure correctly, a good heat exchange being obtained only by a good contact of the thermocouple with the vessel. A comparison of the results for the Ga–As system, shows good agreement between the various authors, except on the Ga-rich side, where the measurements of Van den Boomgaard and Schol [18] were discarded. The same observation applies to the In–As system. On the In-rich side of this system Karataev et al.'s measurements [32] do not agree very well with Pupp, Murray and Pottie's extrapolated values [6]. At high As content, Van den Boomgaard and Schol [18] and Karataev et al. [32] agree very well, the total pressure being higher at the dew-point temperature. We have therefore discarded the metal-rich values of Van den Boomgaard et al. and Karataev et al. for the In–As system.

5.3. The EMF measurements

The reproducibility of the EMF measurements, which is generally about 2×10^{-4}, is only 2×10^{-2} for the GaAs and InAs measurements [27,28,34]. This poor stability may be due either to diffusion and surface phenomena on the two-phase mixtures (GaAs + As or InAs + As), or to unknown parasitic reactions with the electrolyte. In tables 9 and 10, the third law values are systematically higher than the calorimetric determinations and this cannot be explained by the possibility of the existence of low valence states of chlorides in the electrolyte. Lower values of the Gibbs energy could be obtained by Ga or In surface migrations. In the optimization analysis, it was not found that a good convergence was never obtained when these EMF values were used with all the other retained experimental data. Therefore, in the final run, all the EMF values were discarded.

5.4. Calorimetric and heat content measurements

For the InAs compound (table 6), the two [42,43] available enthalpy of formation values differ by 10%. For GaAs, two values are also available [29,35] and these differ by 5%. An accuracy of $\pm 5\%$ is allocated to all these values.

The low temperature heat capacities available are from Piesbergen [36]. For these, the maximum uncertainty is estimated to be $\pm 5\%$. The high temperature C_p values are mainly determined by drop calorimetric measurements [38,40]; the values lie within $\pm 5\%$ of each other for InAs and GaAs. For the GaAs compound, Dash et al. [39] redetermined the heat capacity by differential scanning calorimetry. Their value agrees with those of Lichter and Sommelet [40] and Piesbergen [36] at 300 K. Hence the mean value between Lichter and Sommelet [40] and Dash et al. [39] was retained.

The observation is made for the two compounds that the available heat content values always agree to within 10%. This is generally the accuracy of calorimetric measurements, and indicates that there are probably no parasitic phenomena associated with the determinations.

The enthalpies of fusion have been measured by drop calorimetry [38,40] and deduced from differential thermal analysis [41]. The latter value has been discarded because of the large uncertainty given by the authors.

Table 11
Selected vapor pressure and activity measurements over GaAs and their estimated accuracies

Reference	Method of measurement	Estimated $\Delta P(As_2)/P(As_2)$ (%)	Origin of the uncertainty	Estimated ΔT (K)	Origin of the uncertainty
Drowart and Goldfinger [11]	Knudsen-cell mass spectrometry	±30	Estimated from mass loss calibration and unknown evaporation coefficient	±10	Authors' estimate
Arthur [13]	Knudsen-cell mass spectrometry with a cold trap around the ion source	±20	Estimated from mass loss calibration and residual reevaporation in the source	±10	Author's estimate; calibration with a pyrometer
Foxon et al. [15]	Knudsen-cell mass spectrometry with a cold trap around the ion source and a molecular beam modulator	±30	Estimated from calibration of the mass spectrometer and residual reevaporation in the ion source	±10	Estimated from author's calculations (±3 K) and regulation (±1 K)
Pupp et al. [6]	Knudsen-cell mass spectrometry with a cold trap and a shutter profile	±20	Estimated from calibration procedure and residual reevaporation	±10	Estimated from authors' calibration against In and Pb vapor pressure
Lyons and Silvestri [a] [20]	Dew point method	±20	Estimated from the authors' uncertainties	±3	Estimated from authors' estimate
Van den Boomgaard and Schol [18]	Dew point method	±20	Only high dew point pressures are retained (for $T_{dew\ point} \geq 569°C$) in table II of ref. [18]	±3	Authors' estimate
Rakov et al. [21]	Dew point method and continuous weighing	±20	Estimated; the same experimental conditions as in ref. [18]	±3	Estimated; twice authors' estimate
Richman [22]	Bourdon gauge	±20	Estimated	±3	Author's estimate
Panish [26]	$H_2 + PH_3$ flow method	±20	Estimated	±10	By analogy with InP study as estimated in ref. [1]

[a] As these determinations are far from optimized values, they were discarded in the final treatment.

Table 12
Selected vapor pressure and activity measurements over InAs and their estimated accuracies

Reference	Method of measurement	Estimated $\Delta P(As_2)/P(As_2)$ (%)	Origin of the uncertainty	Estimated ΔT (K)	Origin of the uncertainty
Pupp et al. [6]	Knudsen-cell mass spectrometry with a cold trap and a shutter profile	±50	Estimated from calibration procedure, residual reevaporation and instabilities	±10	Estimated from authors' calibration against In and Pb vapor pressures
Van den Boomgaard and Schol [18]	Dew point method	±20 [a]	Only high dew point pressures are retained (for $T_{dew\ point} \geq 826$ K) in table I of ref. [18]	±4	Authors estimate
Karataev et al. [32]	Dew point method and continuous weighing	±20 [a]	By analogy with ref. [18] we retain only the total pressures for $T_{dew\ point} \geq 826$ K	±2	Estimated; twice authors' estimate

[a] After optimization, the calculated statistical uncertainty is very often close to 20%, and sometimes larger. We thus conclude that the consistency of the selected raw data is not very good.

5.5. Phase diagram determinations: experimental techniques

All the liquidus determinations agree with each other and no analysis of the different techniques is needed to explain the very small differences between the data. We think that the main difference will be revealed when the accuracy of the different determinations is evaluated. For example, the vaporization of As_2 and As_4 or the reaction with H_2 to produce AsH_3 will theoretically slightly shift the liquidus values of Hall [45], Perea and Fonstad [48] and Sol et al. [47] towards the compounds. The same shift occurs with the filtration method [46] since some small crystals may be retained in the liquid. These observations will result in an error which is larger than the author's estimate (see section 6).

Table 13
Selected experimental thermal data for the compound GaAs and their estimated accuracies

Reference	Method of measurement	Thermodynamic data	Value for the compound	Uncertainty	Origin of the uncertainty
Martosudirjo and Pratt [35]	Calorimetric precipitation	Enthalpy of formation (kcal mol^{-1})	$\Delta H_f^\circ(298\ K) = -19.69$	± 1.0	This work ($\pm 5\%$)
Sirota [29]	O_2 calorimetric bomb		$\Delta H_f^\circ(298\ K) = -20.96$	± 1.0	Author's estimate
Piesbergen [36]	Thermometry	Entropy (cal K^{-1} mol^{-1})	$S_{298}^\circ = 15.34$	± 0.8	This work
Holste [37]	Thermometry			($\pm 5\%$)	
Dash et al. [39]	Differential Scanning Calorimetry	Heat capacity (cal K^{-1} mol^{-1})	$C_p = 5.507 + 9.974\ 10^{-4}T$	$\pm 5\%$	This work
Lichter and Sommelet [40]	Drop calorimetry				
Richman and Hockings [41]	Differential Thermal Analysis	Enthalpy of fusion (kcal mol^{-1})	$L_f = 21$	± 5	Author's estimate
Lichter and Sommelet [40]	Drop calorimetry		$L_f = 25.18$	± 1.3 ($\pm 5\%$)	This work

Table 14
Selected experimental thermal data for the compound InAs and their estimated accuracies

Reference	Method of measurement	Thermodynamic data	Value for the compound InAs	Uncertainty	Origin of the uncertainty
Schottky and Bever [42]	Dissolution calorimetry	Enthalpy of formation (kcal mol^{-1})	$\Delta H_f^\circ(298\ K) = -15.1$	± 0.7	This work (see text)
Sharifov and Gadzhiev [43]	Synthesis in a calorimetric bomb		$\Delta H_f^\circ(298\ K) = -13.8$	± 1.0	This work: possibility of its vaporization during synthesis
Piesbergen [36]	Thermometry	Entropy (cal K^{-1} mol^{-1})	$S_{298}^\circ = 18.1$	± 0.9	This work
Holste [37]	Thermometry			(5%)	
Lichter and Sommelet [40]	Drop calorimetry	Heat capacity (cal K^{-1} mol^{-1})	$C_p = 11.822 + 2.026 \times 10^{-3}T$ (298–1215 K)	$\pm 5\%$	This work
Cox and Pool [38]	Drop calorimetry	Enthalpy of fusion (kcal mol^{-1})	$L_f = 18.4$	± 1.8 ($\pm 10\%$)	This work
Lichter and Sommelet [40]	Drop calorimetry		$L_f = 17.58$	± 0.9 (5%)	This work

6. Optimization of thermodynamic and phase diagram data

The analysis of the experimental results enables a selection of raw data which are combined with phase diagram information in an optimization procedure developed by Lukas et al. [56] and based on a least squares analysis. The optimized coefficients of the excess Gibbs energy of the liquid phase, as well as those for the compounds InAs and GaAs are thereby obtained.

The Gibbs energy of formation of the compound is given by the following equation:

$$\Delta G_f^\circ = a - bT + cT(1 - \ln T) - \frac{dT^2}{2} - \frac{e}{2T}. \quad (12)$$

The excess Gibbs energy of the liquid solution phase is described by the general expression:

$$\Delta G^{xs} = x(1-x) \sum_{\nu=0}^{\nu=n} a_\nu (1-2x)^\nu. \quad (13)$$

When $\nu = 0$ the expression corresponds to that derived from the regular solution model. Moreover, if a_0 is temperature dependent, ΔG^{xs} will describe the thermodynamic properties of mixing according to a 'simple solution model' [58].

The thermodynamic properties of pure In and Ga are taken from Hultgren et al's compilations [3]. In the experiments, it is the partial pressures of As_2 or As_4, or the total pressure, which has been measured in equilibrium with InAs or GaAs. Activity data may therefore be derived either from the directly measured As_2 or As_4 pressures, or from those derived from total pressure determinations. As the As_2 pressures seem more accurate at low pressures, these were used to recalculate activity data in the whole temperature range of the measurements.

The optimization procedure was made using $0 \leqslant \nu \leqslant 2$. The criteria for the best choice of ν is the ratio between experimental accuracies and calculated uncertainties together with the convergency coefficient. This coefficient is the standard deviation for all the data, each of them being weighted by its experimental estimated accuracy. As a general rule, the minimum set of parameters is preferable. The experimental accuracies are pro-

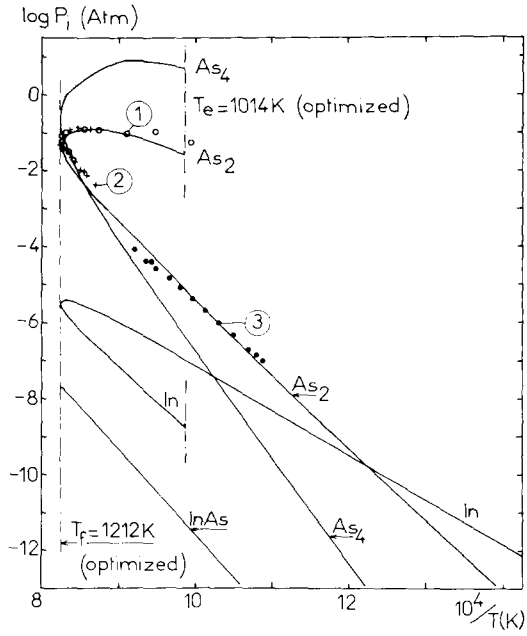

Fig. 8. Optimized partial pressures of As_2, As_4, In and InAs gaseous species along the liquidus in the In–As system and selected experimental data: (1) Van den Boomgaard and Schol [18]; (2) Karataev et al. [32]; (3) Pupp et al. [6].

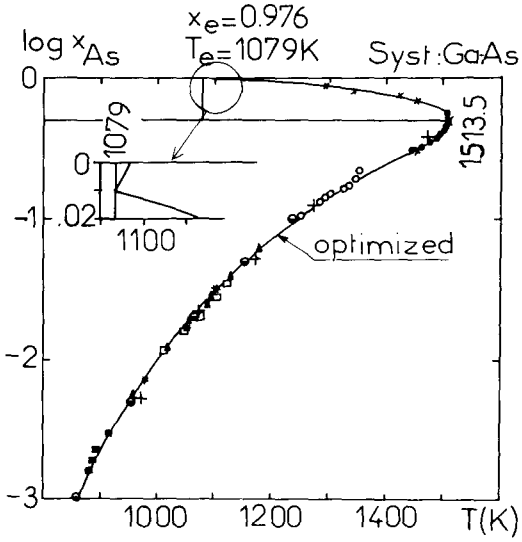

Fig. 9. Optimized phase diagram of the Ga–As system and selected experimental data: (×) Koster and Thoma [44]; (●) Rakov et al. [21]; (+) Rubenstein [46]; (○) Vigdorovich et al. [8]; (◒) Hall [45]; (▲) Hsieh [23], (□) Sol et al. [47]; (■) Perea and Fonstad [48].

Table 15
Selected phase diagram determinations for the Ga–As system and their estimated accuracies

Reference	Method of measurement	Estimated uncertainty $\Delta x_{As}/x_{As}$	Origin of the uncertainty	Estimated ΔT (K)	Origin of the uncertainty
Goldsmith in Koster and Thoma [44]	Differential Thermal Analysis	±0.01	Weight of the initial components and As in the vapor phase	±10	Estimated from possibility of undercooling
Richman and Hockings [41]	Differential Thermal Analysis at the melting point of GaAs (1518 K)	±0.01	Weight of the initial components and As in the vapor phase	±5	Authors' estimate
Rubenstein [46]	Filtration technique	+0.01 (±0.05) −0.10	Author's estimate and possibility of retaining some small crystals	±10	This work
Rakov et al. [21]	Dew point and continuous weighing	±0.01	Uncertainties in the temperature distribution in the vessel and the choice of $K_P(As_4 \rightleftharpoons 2\ As_2)$	±3	This work: twice the authors' estimate
Vigdorovich et al. [8]	Bourdon gauge and vapor density	±0.01	This work	±10	This work
Hall [45]	Heterogeneous equilibrium and single crystal weight loss	+0.01 (±0.02) −0.03	Possibility of As loss by vapor phase	±10	Author's estimate
Sol et al. [47]	Heterogeneous equilibrium in a LPE reactor and single crystal weight loss	±0.01	This work	±5 [a]	This work
Perea and Fonstad [48]	Heterogeneous equilibrium in a LPE reactor and single crystal weight loss	±0.01	This work: twice authors' estimate	±5 [a]	This work
Hsieh [23]	–	±0.01	This work	±10	This work
Dutartre [59]	Visual observation of crystals	±0.02	This work	±3	Author's estimate

[a] See ref. [1].

Table 16
Selected experimental phase diagram determinations for the In–As system and their estimated accuracies

Reference	Method of measurement	Estimated uncertainty $\Delta x_{As}/x_{As}$	Origin of the uncertainty	Estimated ΔT (K)	Origin of the uncertainty
Liu and Peretti [49]	Differential Thermal Analysis	±0.01 (±0.03) −0.05	$x_{As} < 0.5$: As loss by vapor	±5	Authors' estimate and possibility of undercooling
		±0.01	$x_{As} > 0.5$: this work		
Karataev et al. [32]	Dew point and continuous weighing	±0.01	Uncertainty in the temperature distribution and error in the $K_P(As_4 \rightleftharpoons 2\ As_2)$	±2	Estimated: twice the authors' estimate
Hall [45]	Weight loss of a single crystal	+0.01 (±0.02) −0.03	Possibility of As loss by the vapor phase	±3	Author's estimate
Perea and Fonstad [48]	Heterogeneous equilibrium in a LPE reactor and weight loss of a single crystal	±0.01	Estimated: twice the authors' estimate	±5 [a]	This work

[a] See ref. [1].

Table 17
Optimized thermodynamic data for the compounds GaAs and InAs and comparison with selected experimental raw data

System	Thermodynamic functions	Selected experimental data	Optimized values	Mean difference or $\lvert opt - exp \rvert / \lvert opt \rvert$
Ga–As [a]	Mixing properties of the liquid (Ga_xAs_{1-x})	No data	"Simple solution" $\alpha = 376.2 - 5.983T$ (cal mol^{-1})	
	$\Delta C_p = 0$ $\Delta G_f(GaAs, s) = a - bT$ (convergency coefficient = 1.2) Ga(s or l) + As(s or l) $\rightleftharpoons$ GaAs(s)	From ref. [39,40] Vapor pressure from refs. [11,13,15,6,18,21,22,26]	$a = -19537$ (s.d. ± 12) (cal mol^{-1}) $b = -1.849$ (s.d. $\pm 8.6 \times 10^{-6}$) (cal mol^{-1})	Mean deviation $\Delta P(As_2)/P(As_2)$ $= \pm 40\%$ for 156 values
	ΔH_f°(GaAs, s, 298 K) Ga(s) + As(s) $\rightleftharpoons$ GaAs(s)	-19.69 kcal mol^{-1} [35] -20.96 kcal mol^{-1} [29]	-19.54 (± 0.30) kcal mol^{-1}	$+1\%$ $+7\%$
	S_{298}°(GaAs, s)	15.34 cal K^{-1} mol^{-1} [36]	16.05 (± 0.8) kcal mol^{-1}	4.4%
	L_f(GaAs, s $\rightarrow$ l) $T_f = 1513.5 \pm 3$ K (opt.)	21 kcal mol^{-1} [41] 25.18 kcal mol^{-1} [40]	27.0 (± 0.8) kcal mol^{-1}	$+22\%$ $+7\%$
In–As [b]	Mixing properties of the liquid	No data	"Simple solution" $\alpha = -3944 - 2.346T$ (cal mol^{-1})	
	$\Delta C_p = 0$ $\Delta G_f(InAs, s) = a - bT$ (convergency coefficient = 1.7) In(s or l) + As(s or l) $\rightleftharpoons$ InAs	From ref. [41] Vapor pressures from refs. [6,18,32]	$a = -14291$ (s.d. ± 8.4) (cal mol^{-1}) $b = -2.257$ (s.d $\pm 6 \times 10^{-6}$) (cal mol^{-1})	Mean deviation $\Delta P(As_2)/P(As_2)$ $= \pm 25\%$ for 34 values
	ΔH_f°(InAs, s, 298 K) In(s) + As(s) $\rightleftharpoons$ InAs(s)	-15.1 kcal mol^{-1} [42] -13.8 kcal mol^{-1} [43]	-14.29 (± 0.50) kcal mol^{-1}	-5.7% -3.5%
	S_{298}°(InAs, s)	18.1 cal K^{-1} mol^{-1} [36]	17.84 (± 0.8) cal K^{-1} mol^{-1}	1.4%
	L_f(InAs, s $\rightarrow$ l) $T_f = 1212 \pm 3$ K (opt.)	18.4 kcal mol^{-1} [38] 17.58 kcal mol^{-1} [40]	19.04 (± 1.00) kcal mol^{-1}	-3.4% $+7.7\%$

[a] Standard Ga [3]; standard As, see section 2.
[b] Standard in [3]; standard As, see section 2.

Table 18
Optimized values for the liquidus composition and vapor pressures along the liquidus in the Ga–As system

Temperature (K)	Molar fraction of As, x_{AS} (at%)	Vapor pressures (atm)			
		As_2	As_4	Ga	Total
800	0.0308	4.47×10^{-14}	2.00×10^{-20}	2.11×10^{-12}	2.15×10^{-12}
850	0.0859	1.53×10^{-12}	3.05×10^{-18}	2.24×10^{-11}	2.39×10^{-11}
900	0.213	4.24×10^{-11}	4.03×10^{-16}	1.84×10^{-10}	2.26×10^{-10}
950	0.478	5.12×10^{-10}	2.33×10^{-14}	1.18×10^{-9}	1.69×10^{-9}
1000	0.976	9.44×10^{-9}	9.98×10^{-13}	6.25×10^{-9}	1.57×10^{-8}
1050	1.83	9.79×10^{-8}	2.96×10^{-11}	2.83×10^{-8}	1.26×10^{-7}
1100	3.15	7.98×10^{-7}	6.35×10^{-10}	1.08×10^{-7}	9.06×10^{-7}
1150	5.03	4.58×10^{-6}	7.05×10^{-9}	3.75×10^{-7}	4.97×10^{-6}
1200	7.52	2.26×10^{-5}	6.46×10^{-8}	1.17×10^{-6}	2.39×10^{-5}
1250	10.61	1.01×10^{-4}	5.20×10^{-7}	3.14×10^{-6}	1.05×10^{-4}
1300	14.33	4.10×10^{-4}	3.84×10^{-6}	8.05×10^{-6}	4.21×10^{-4}
1350	18.72	1.56×10^{-3}	3.01×10^{-5}	1.83×10^{-5}	1.61×10^{-3}
1400	23.97	6.37×10^{-3}	2.15×10^{-4}	3.58×10^{-5}	6.59×10^{-3}
1450	30.60	2.67×10^{-2}	1.89×10^{-3}	6.18×10^{-5}	2.68×10^{-2}
1500	41.10	0.154	3.35×10^{-2}	8.75×10^{-5}	0.188
1513.5	50.00	0.457	0.248	7.01×10^{-5}	0.705
1500	58.90	0.957	0.774	3.52×10^{-5}	1.73
1450	69.40	1.51	6.08	8.20×10^{-6}	7.59
1400	76.03	1.58	13.21	2.27×10^{-6}	14.79
1350	81.28	1.35	19.32	6.22×10^{-7}	20.67
1300	85.67	1.12	28.97	1.54×10^{-7}	30.09
1250	89.38	0.836	35.73	3.44×10^{-8}	36.57
1200	92.48	0.562	39.81	7.43×10^{-9}	40.37
1150	94.97	0.343	40.18	1.36×10^{-9}	40.52
1100	96.85	0.191	36.48	2.21×10^{-10}	36.67
1079 (eut.)	97.60	0.150	29.85	3.55×10^{-11}	30.00
1090	100.0	0.176	37.47	0.0	37.65
$\Delta T = \pm 5.6$ K [a]	$\Delta x_{As} = 0.9\%$ [a]	$\Delta P/P = 40\%$ [a]			

[a] This mean deviation corresponds to the statistical maximum uncertainty for each of the parameters T, x or P when the uncertainties of the two others are set equal to zero.

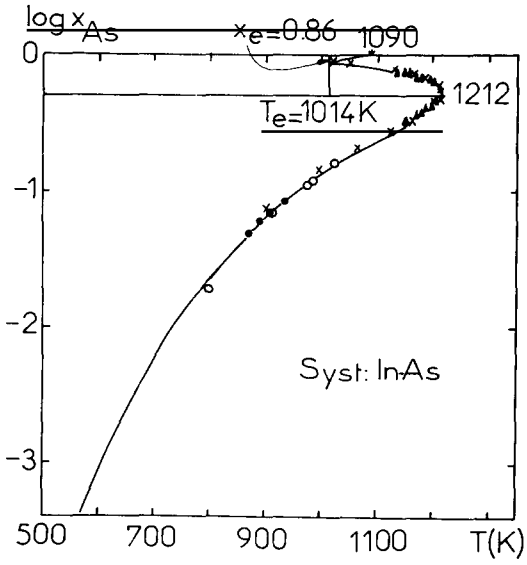

Fig. 10. Optimized phase diagram of the In–As system and selected experimental data: (×) Liu and Peretti [49]; (▲) Karataev et al. [32]; (○) Hall [45]; (●) Perea and Fonstad [48].

vided either by the author, or have been estimated in this work, as presented in tables 11 to 16. The raw data which are retained for the optimization are selected according to the thermodynamic and methodological analysis described in sections 3 and 4. In this analysis, the equations describing the heat capacity of GaAs and InAs were selected from calorimetric determinations after noting that calculation of the coefficients a, b, c and d of eq. (12) by the optimization procedure led to less

Table 19
Optimized values for the liquidus composition and vapor pressures along the liquidus in the In–As system

Temperature (K)	Molar fraction of As, x_{As} (at%)	Vapor pressures (atm)			
		As_2	As_4	In	Total
600	0.0734	8.24×10^{-19}	4.81×10^{-25}	5.43×10^{-16}	5.44×10^{-16}
650	0.219	2.09×10^{-16}	9.77×10^{-22}	2.06×10^{-14}	2.08×10^{-14}
700	0.550	2.34×10^{-14}	6.52×10^{-19}	4.71×10^{-13}	4.94×10^{-13}
750	1.197	1.50×10^{-12}	2.00×10^{-16}	7.00×10^{-12}	8.50×10^{-12}
800	2.301	5.48×10^{-11}	3.01×10^{-14}	7.31×10^{-11}	1.28×10^{-10}
850	3.971	1.41×10^{-9}	2.60×10^{-12}	6.03×10^{-10}	2.01×10^{-9}
900	6.267	2.58×10^{-8}	1.48×10^{-10}	3.68×10^{-9}	2.96×10^{-8}
950	9.212	3.51×10^{-7}	5.64×10^{-9}	1.87×10^{-8}	3.75×10^{-7}
1000	12.83	3.78×10^{-6}	1.61×10^{-7}	7.55×10^{-8}	4.02×10^{-6}
1050	17.21	3.68×10^{-5}	4.09×10^{-6}	2.27×10^{-7}	4.12×10^{-5}
1100	22.57	2.98×10^{-4}	2.11×10^{-5}	8.00×10^{-7}	3.20×10^{-4}
1150	29.50	1.87×10^{-3}	2.19×10^{-3}	2.01×10^{-6}	3.06×10^{-3}
1200	40.87	1.57×10^{-2}	3.09×10^{-2}	3.90×10^{-6}	4.66×10^{-2}
1212	50.00	3.62×10^{-2}	0.208	3.26×10^{-6}	0.244
1200	59.13	9.23×10^{-2}	1.07	1.61×10^{-6}	1.16
1150	70.50	0.116	4.57	2.56×10^{-7}	4.69
1100	77.43	9.27×10^{-2}	8.11	4.54×10^{-8}	8.20
1050	82.78	4.78×10^{-2}	6.87	7.45×10^{-9}	6.92
1014 (eut.)	86.37	2.51×10^{-2}	6.68	1.68×10^{-9}	6.70
1090	100	0.176	37.47	0.0	37.65
$\Delta T = \pm 10$ K [a]	$\Delta x = \pm 2.7\%$ [a]	$\Delta P/P = \pm 25\%$ [a]			

[a] This mean deviation corresponds to the statistical maximum uncertainty for each of parameters T, x or P when the uncertainties of the two other are set equal to zero.

satisfactory results. This selection corresponds in fact to $\Delta C_p \sim 0$. The analysis shows that the thermodynamic behavior of the liquid solution can be described by a "simple solution model" [58]. Table 17 presents the optimized set of data, consistent with the phase diagram, for both systems. Figs. 7 to 9 shows the vapor composition in equilibrium with the compounds and the phase diagram resulting from the optimization. For the Ga–As system, the set of raw data is highly consistent. The experimental values already selected by Shaw [63] for the GaAs compound have also been selected as raw data in our analysis. So these values are close to our optimized one. For the In–As system, the raw data are scarce, and more complete determinations, especially at intermediate temperatures, are needed. Discrete values along the liquidus are presented in tables 18 and 19.The small differences from the results obtained previously by Dutartre et al. [59–61] for Ga–As arise from the fact that as a result of discarding the raw vapor pressure data, their set of basic data was more limited.

Acknowledgements

The authors are grateful to Dr. L. Lukas for the use of this optimization program and to Dr. M. Rand and Dr. P.J. Spencer for their fruitful discussions.

References

[1] M. Tmar, A. Gabriel, C. Chatillon and I. Ansara, J. Crystal Growth 68 (1984) 557.
[2] D.R. Stull and G.C. Sinke, Thermodynamic Properties of Elements (Am. Chem. Soc., Washington, DC, 1956).
[3] R. Hultgren, P.D. Desai, D.T. Hawkins, M. Gleiser, K.K. Kelley and D.D. Wagman, Selected Values of the Thermodynamic Properties of the Elements (Am. Soc. Metals, Metals Park, OH, 1973).

[4] J. Drowart, private communication (1977) to Thermodata.
[5] J.J. Murray, C. Pupp and R.F. Pottie, J. Chem. Phys. 58 (1973) 2569.
[6] C. Pupp, J.J. Murray and R.F. Pottie, J. Chem. Thermodyn. 6 (1974) 123.
[7] J. Drowart, S. Smoes and A. Vanderauwera-Mahieu, J. Chem. Thermodyn. 10 (1978) 453.
[8] E.N. Vigdorovich, V.V. Popov, M.M. Artamonov and V.M. Andreev, Izv. Akad. Nauk SSSR Neorg. Mater. 9 (1973) 771.
[9] H. Rau, J. Chem. Thermodyn. 7 (1975) 27.
[10] L. Kaufman, J. Nell, K. Taylor and F. Hayes, Calphad 5 (1981) 185.
[11] J. Drowart and P. Goldfinger, J. Chim. Physique 55 (1958) 721.
[12] H.B. Gutbier, Z. Naturforsch. 16a (1961) 268.
[13] J.R. Arthur, J. Phys. Chem. Solids 28 (1967) 2257.
[14] G. De Maria, L. Malaspina and V. Piacente, J. Chem. Phys. 52 (1970) 1019.
[15] C.T. Foxon, J.A. Harvey and B.A. Joyce, J. Phys. Chem. Solids 34 (1973) 1693.
[16] C.T. Foxon, B.A. Joyce, R.F.C. Farrow and R.M. Griffiths, J. Phys. D. (Appl. Phys.) 7 (1974) 2422.
[17] R.N. Rubinshteiin and V.M. Kozlovskaya, cited in ref. [29].
[18] J. van den Boomgaard and K. Schol, Philips Res. Rept. 12 (1957) 127.
[19] O.G. Folberth, Z. Naturforsch. 13a (1958) 856.
[20] V.J. Lyons and V.J. Silvestri, J. Phys. Chem. 65 (1961) 1275.
[21] V.V. Rakov, B.D. Lainer and M.G. Mil'vidskii, Russ. J. Phys. Chem. 44 (1970) 922.
[22] D. Richman, J. Phys. Chem. Solids 24 (1963) 1131.
[23] J.J. Hsieh, cited by R.F. Brebrick, Met. Trans. 8A (1977) 403.
[24] Yu. P. Khukhryanskii, V.P. Kondaurov, F.P. Nikolaeva, V.I. Panteleev and M.I. Shshevelev, Izv. Akad. Nauk SSSR Neorg. Mater. 10 (1974) 1877.
[25] Yu.P. Khukhryanskii, V.P. Kondaurov, F.P. Nikolaeva and V.I. Panteleev, Russ. J. Phys. Chem. 48 (1974) 909.
[26] M.B. Panish, J. Crystal Growth 27 (1974) 6.
[27] A.S. Abbasov, K.N. Mamedov, A.V. Nikol'skaya, Ya.I. Gerasimov and V.P. Vasil'ev, Dokl. Akad. Nauk SSSR 170 (1966) 1238.
[28] A.N. Krestovnikov, V.B. Ufimtsev and E.M. Solopai, Russ, J. Phys. Chem. 45 (1971) 1504.
[29] N.N. Sirota, in: Semiconductors and Semimetals, Vol. 4, Eds. R.K. Willardson and A.C. Beer (Academic Press, New York, 1968) ch. 2, pp. 35–162.
[30] H.B. Gutbier, Z. Naturforsch. 14a (1959) 32.
[31] P. Goldfinger and M. Jeunehomme, in: Advances in Mass Spectrometry, Vol. 1 (Pergamon, London, 1959) p. 534.
[32] V.V. Karataev, M.G. Mil'vidskii, G.A. Nemtsova, V.V. Rakov and I.A. Dolgikh, Izv. Akad. Nauk SSSR Neorg. Mater. 11 (1973) 830.
[33] Yu.P. Khukhryanskii and V.I. Panteleev, Russ, J. Phys. Chem. 51 (1977) 1275.
[34] A.S. Abbasov, A.V. Nikol'skaya, Ya. I. Gerasimov and V.P. Vasil'ev, Dokl. Akad. Nauk SSSR 156 (1964) 118.
[35] S. Martosudirjo and J.N. Pratt, Thermochim. Acta 10 (1974) 23.
[36] U. Piesbergen, Z. Naturforsch. 18a (1963) 141.
[37] J.C. Holste, Phys. Rev. B6 (1972) 2495.
[38] R.H. Cox and J. Pool, J. Chem. Eng. Data 12 (1967) 247.
[39] A.J. Dash, A. Finch and P.J. Gardner, J. Chem. Eng. Data 19 (1974) 113.
[40] B.D. Lichter and P. Sommelet, Trans. Met. Soc. AIME 245 (1969) 1021.
[41] D. Richman and E.F. Hockings, J. Electrochemical Soc. 112 (1965) 461.
[42] W.F. Schottky and M.B. Bever, Acta Met. 6 (1958) 320.
[43] K.A. Sharifov, S.N. Gadzhiev and I.M. Garibov, Izv. Akad. Nauk Azerb. SSR Ser. Fiz. Mat. Tekhn. Nauk 2 (1963) 53, cited in ref. [29].
[44] W. Koster and B. Thoma, Z. Metallk. 46 (1955) 291.
[45] R.N. Hall, J. Electrochem. Soc. 110 (1963) 385.
[46] M. Rubenstein, J. Electrochem. Soc. 113 (1966) 752.
[47] N. Sol, J.P. Clariou, N.T. Linh and M. Moulin, J. Crystal Growth 27 (1974) 325.
[48] E.H. Perea and C.G. Fonstad, J. Electrochem. Soc. 127 (1980) 313.
[49] T.S. Liu and E.A. Peretti, Trans. Am. Soc. Metals 45 (1953) 677.
[50] V. Piacente and R. Gigli, J. Chem. Phys. 77 (1982) 4790.
[51] M. Brewer and G. Rosenblatt, in: Advances in High Temperature Chemistry, Vol. 2 (Academic Press, New York, 1969) pp. 1–74.
[52] M. Tmar, A. Pasturel and C. Colinet, J. Chem. Thermodyn. 15 (1983) 1037.
[53] C. Chatillon, M. Allibert and A. Pattoret, High Temp. Sci. 8 (1976) 233.
[54] J.S. Kane and J.H. Reynolds, J. Chem. Phys. 25 (1956) 342.
[55] C.Y. Lou and G.A. Somorjai, J. Chem. Phys. 55 (1971) 4554.
[56] H.L. Lukas, E. Th. Henig and B. Zimmermann, Calphad 1 (1977) 225.
[57] P. Dorner, E. Th. Henig, H. Krieg, H.L. Lukas and G. Petzow, Calphad 4 (1980) 241.
[58] E.A. Guggenheim, Thermodynamics (North-Holland, Amsterdam, 1967) pp. 196–200.
[59] D. Dutartre, Thesis, INSA, Lyon (1983).
[60] D. Dutartre, M. Gavand, L. Mayet, A. Laugier and I. Ansara, J. Physique 43 Suppl. 121 (1982) C5-39.
[61] D. Dutartre and I. Ansara, Calphad, to be published.
[62] M.E. Weiner, J. Electrochem. Soc. 119 (1972) 496.
[63] D.W. Shaw, J. Phys. Chem. Solids 36 (1975) 111.
[64] V.S. Ban, J. Electrochem. Soc. 118 (1971) 1473.